





Meta-heuristic optimization for drying kinetics and quality assessment of *Capparis spinosa* buds

Chafika Lakhdari, Hocine Remini, Nourelimane Benzitoune, Samia Djellal, Mohamed Hentabli, Meriem Adouane, Farid Dahmoune & Nabil Kadri


To cite this article: Chafika Lakhdari, Hocine Remini, Nourelimane Benzitoune, Samia Djellal, Mohamed Hentabli, Meriem Adouane, Farid Dahmoune & Nabil Kadri (11 Aug 2024): Meta-heuristic optimization for drying kinetics and quality assessment of *Capparis spinosa* buds, Chemical Engineering Communications, DOI: [10.1080/00986445.2024.2389154](https://doi.org/10.1080/00986445.2024.2389154)

To link to this article: <https://doi.org/10.1080/00986445.2024.2389154>

 View supplementary material [↗](#)

 Published online: 11 Aug 2024.

 Submit your article to this journal [↗](#)

 View related articles [↗](#)

 View Crossmark data [↗](#)



Meta-heuristic optimization for drying kinetics and quality assessment of *Capparis spinosa* buds

Chafika Lakhdari^a, Hocine Remini^{b,c}, Nourelimane Benzitoune^a, Samia Djellal^a, Mohamed Hentabli^d, Meriem Adouane^a, Farid Dahmoune^{b,c}, and Nabil Kadri^{b,c}

^aLaboratoire de Gestion et Valorisation des Ressources Naturelles et Assurance Qualité (LGVRNAQ), Faculté des Sciences de la Nature et de la Vie et des Sciences de la Terre, Université de Bouira, Bouira, Algeria; ^bDépartement de Biologie, Faculté des Sciences de la Nature et de la Vie et des Sciences de la Terre, Université de Bouira, Bouira, Algeria; ^cLaboratoire de Biomathématiques, Biophysique, Biochimie, et Scientométrie (L3BS), Faculté des Sciences de la Nature et de la Vie, Université de Bejaia, Bejaia, Algeria; ^dLaboratory of Biomaterials and Transport Phenomena (LBMP), Faculty of Technology, University Yahia Fares of Médéa, Médéa, Algeria

ABSTRACT

This paper was conducted to model the drying kinetics of *Capparis spinosa* buds using dragonfly swarm optimized nonlinear regression and to compare the impact of drying treatments on their quality. Experiments included hot-air convective drying (HACD) from 40 to 120 °C, vacuum drying (VD) at 40, 60, and 80 °C, microwave drying (MD) ranging from 200 to 1000 W. Out of 30 models tested, the drying kinetics fitted best with Jena Das model in both HACD and VD and modified Midilli for MD. The comparison between the drying treatments used indicated that when taking into account the quality of the dried caper, VD at 80 °C was the most effective, resulting in a high-quality caper with a well-preserved color ($\Delta E = 7.47$), high bioactives (TPC = 30.18 mg GAE/g DW and TFC = 10.27 mg QE/g DW) and radical scavenging abilities (DPPH = 0.249 and ABTS = 4.448 mg/mL) at the expense of long duration (6 h) and high specific energy consumption (50.667 kWh/kg). On the other hand, when considering the drying behavior MD ranked best with samples dried at 1000 W showing high diffusivities $2.04 \times 10^{-8} \text{ m}^2 \text{ s}^{-1}$ low energy consumption (MER 0.1216 kg/h), and short drying times (12 mn). This research is critical in selecting better drying conditions for increased usage in the culinary, cosmetic, and pharmaceutical sectors.

KEYWORDS



Caper; *Capparis spinosa*; dragonfly algorithm; drying; energy efficiency; modeling


Introduction

Plants are excellent suppliers of vitamins, minerals, phenolics, and various vital bioactive substances. They are employed in the creation of functional foods, medications, and other products in addition to folk medicine (Banwo et al. 2021). Capers are the flower-buds of the *Capparis* genus in the *Capparaceae* family, a plant of tropical/subtropical and arid areas.

Capers have been utilized for various purposes since ancient times, and they have thrived naturally across diverse regions of the globe. The buds of the *Capparis spinosa* plant are fermented in brine and incorporated into pasta, meat, salads, and other dishes to enhance flavor or serve as an appetizer alongside cheese, olives, and almonds

(Grimalt et al. 2022). Notably, the buds and leaves of the caper plant have found applications in medicine, cosmetics, and cuisine due to their abundance in bioactive compounds with functional attributes (Tayiroğlu and İncedayı 2021). These compounds encompass flavonols, phenolic acids, sugars, alkaloids (Khanavi et al. 2020; Aksay et al. 2021), phytosterols, vitamins, and glucosinolates (Saleem et al. 2021). According to Grimalt et al. (2022), Capers are also renowned in traditional medicine for their astringent, diuretic, tonic, and antirheumatic effects. Many studies have demonstrated their anti-inflammatory effect (Yatao et al. 2021) antihepatotoxic, anti-cancer (Ali et al. 2023) antihyperglycemic effects (Assadi et al. 2021).

CONTACT Lakhdari Chafika  ch.lakhdari@univ-bouira.dz  Laboratoire de Gestion et Valorisation des Ressources Naturelles et Assurance Qualité (LGVRNAQ), Faculté des Sciences de la Nature et de la Vie et des Sciences de la Terre, Université de Bouira, Bouira, 10000, Algeria.

 Supplemental data for this article is available online at <https://doi.org/10.1080/00986445.2024.2389154>

© 2024 Taylor & Francis Group, LLC

The high water content of fresh capers, representing around 80% (wb) (Cincotta et al. 2022). Renders them vulnerable to the growth of undesirable spoilage microorganisms and chemical deterioration which results in shorter shelf life.

Drying is a vital operation in a variety of processing sectors, including chemical, food, pharmaceutical, agricultural, biotechnology, and polymer. Drying is required for safe preservation, simple handling, extended storage, and lower transportation costs. This procedure often implies heating water to reduce its volume. Inadequate dehydration can result in unrecoverable destruction of ultimate product quality, overestimated requirements of time and energy, out-of-season costs, etc. (Solchansanj and Jayas 2020).

Food can be dried using different techniques in the food industry, such as microwave drying, convective dehydration, sun drying, lyophilization, infrared radiation, and vacuum drying (Reis et al. 2022).

Drying with hot air convection ovens is common and essential for postharvest conservation. It has been used to dehydrates many fruits and vegetables, for example, Kittibunchakul et al. dried maoberry fruits and examined the impact of convective drying on bioactive compounds, antioxidant potential, and safe consumption (Kittibunchakul et al. 2023), other recent studies included banana slices (Granella et al. 2022), orange peel (Bechlin et al. 2020), apple slices (Joardder and Karim 2022), and melon slices (Tepe and Kadakal 2022).

However, due to its extended drying times, which may reduce the quality of dried goods and its high energy requirements. Hot-air convection drying (HACD) has been avoided (Oyinloye and Yoon 2020).

Vacuum drying is used to improve quality and nutrition, overcoming the drawbacks of hot air-drying. It efficiently removes water under low pressure, offering faster drying, lower temperatures, and an oxygen-free environment (Shen Y et al. 2021). Different food products have been dried with vacuum driers including red beetroot (*Beta vulgaris*) (Kerr and Varner 2020), carrot and potato (Calín-Sánchez et al. 2020), avocado

by-products (Marović et al. 2024), and okra (*Abelmoschus esculentus*) (Yuan et al. 2020).

Furthermore, microwave drying is a technique that is becoming more and more popular due to its intrinsic benefits over traditional heating, such as its ability to speed up the drying of biological material without sacrificing quality (Tepe and Tepe 2020). Many researches have extensively employed microwave to dry food items, such as blood orange slices (Abderrahim et al. 2022), apple slices (Tepe and Tepe 2020), brown rice (Shen L et al. 2021), barley malt (Carvalho et al. 2021), pistachio kernel (Jahanbakhshi et al. 2020), and kiwi and pepino fruits (Özcan et al. 2020).

Monitoring variations in moisture content as a function of time can be used to explain the drying behavior of agricultural products. Thin-layer drying is the most often used method for a variety of agricultural items. Several mathematical models for thin-layer drying have been proposed by various researchers. To describe the thin-layer drying process, laboratory-based modeling is necessary, which will assist in decreasing energy consumption and optimizing drying equipment design (Buzrul 2022).

Numerous mathematical models have been created, among which thin-layer drying models are prevalent. These models are typically classified into theoretical, semi-theoretical, and empirical categories. Several research studies have focused on investigating drying kinetics and employing thin-layer drying models for various fruits and vegetables.

Khadidja et al. investigated convective and microwave drying of blood oranges. And found that Sledz et al. and Midilli and Kucuk models are the most adequate to fit the drying kinetics (Abderrahim et al. 2022). The drying curves of pistachio nuts were evaluated using six thin-layer drying models (Thompson model, two term exponential model, diffusion model, exponential model, modified Page model, and Page model) (Mokhtarian et al. 2021). Using the Page, Midilli, and Küçük models as well as the Modified Page model, Arslan and Özcan examined the experimental data of drying onion slices, red bell pepper slices, and rosemary leaves in the sun, oven, and microwave (Arslan et al. 2020; Horuz et al. 2020). Microwave drying kinetics of white

mulberry were examined using five thin-layer drying models including Lewis, Henderson, and Pabis, page, Wang and Singh, and Midilli et al. (Kipcak and Doymaz 2020). Ten models, including Midilli equations, Two-term exponential, Two-term, Verma, Diffusion, Wang and Singh, logarithmic, Henderson, Page, and Newton were used by Simha et al. to study the dehydration of some medicinal plants by microwave (Kant et al. 2023).

The dehydration procedure can cause a degradation in the quality of the material, particularly for substances sensitive to heat, light, and oxygen, such as phytochemicals. Researchers often monitor these compounds throughout the drying process to ensure their preservation and maintain the highest possible product quality.

Several studies have reported that capers (*Capparis spinosa* buds) are an abundant source of total phenolics and flavonoids. For example, Elshibani et al. (2020) found that *Capparis spinosa* buds contain 555 ± 0.5 mg GAE/g of total phenolic content (TPC) and 102.59 ± 0.6 mg QE/g of flavonoids, with an IC₅₀ value of 0.07 ± 0.02 mg/mL for DPPH radical scavenging activity (Elshibani et al. 2020). Yahia et al. (2020) also evaluated the bioactive content and antioxidant activity of *Capparis spinosa* extract, reporting TPC and flavonoid contents of 12.58 mg GAE/g and 1.60 mg QE/g, respectively. This study identified quinic acid, gallic acid, protocatechuic acid, and catechin as the predominant phenolic acids, with catechin being the most abundant flavonoid. Additionally, strong antioxidant activities were observed, with EC₅₀ values of 74.02 mg/mL and 150.26 mg/mL using the DPPH and ABTS assays, respectively (Yahia et al. 2020).

Regarding the color of caper flower buds, which can serve as an indicator of processing conditions, Tayiroğlu and İncedayı reported color values predominantly in greenness ($-a^*$) and yellowness (b^*) tones (Tayiroğlu and İncedayı 2021).

Aksay et al. further described the color of caper buds as bright green, with L^* (lightness) value of 9.38 ± 0.22 , an a^* (redness) value of -4.29 ± 0.02 , and a b^* (yellowness) value of 8.10 ± 0.11 (Aksay et al. 2021).

Yayuan Xua et al. compared the retention of chlorophyll, phenolics, flavonoids, and antioxidant activities (ABTS, DPPH, and ORAC) of cabbage under various dehydrating treatments. He came to the conclusion that MVD in combination with HAD or VD showed superior antioxidant activity and nutritional composition preservation (Xu et al. 2020).

Méndez-Lagunas et al. evaluated the effect of convective drying of strawberries on total phenolic compound content (TPC), anthocyanins (A), and antioxidant activity (AA) in addition to the final color change (López-Ortiz et al. 2020). Also, another study made on bananas drying indicated that while lyophilization reduced the phenolic content to a lesser amount, air drying at 50 and 70 °C reduced antioxidant activity and total phenols (Zhou et al. 2022).

As far as our understanding goes, there has been no prior research conducted regarding the drying of *Capparis* buds with the different methods used in our study. Only oven drying was employed to dehydrate *Capparis spinosa* flower buds at 40, 50 °C (Cincotta et al. 2022) and at 50, 60, and 70 °C using four mathematical models namely, page, lewis, logarithmic, and fick (Demir et al. 2023). Therefore, this paper aimed to study and compare the impact of several dehydrating techniques on the quality characteristics of caper flower buds, model the dehydration kinetics, and compute diffusivity, activation energy, and energy efficiency of the buds for the entire operational range.

The findings of this study would make a substantial contribution and provide a scientific foundation for the drying of caper buds, which would then be employed in culinary applications, cosmetics, and pharmaceuticals.

Materials and methods

Material preparation

The flower buds of *Capparis spinosa* were manually harvested from wild plants grown in Medea (North of Algeria) in June 2020. The buds were cleaned, sorted, and calibrated according to their size. Capers of 0.9 ± 0.1 cm in diameter were used in this work. The initial moisture content of fresh

capers ($83.61 \pm 0.27\%$ w.b) was obtained with the oven-drying method (Nirmaan et al. 2020). Three sets of samples were subjected to drying in an oven at a consistent temperature of $103 \pm 2^\circ\text{C}$ until a stable weight was achieved.

Drying processes

Drying treatments were performed using three methods: hot-air convective drying (HACD), microwave drying (MD), and vacuum drying (VD).

Samples of 90 g were spread on one layer in a tray. Moisture loss in the samples was measured on a regular basis by removing the tray and weighing it on a digital balance with 0.01 g precision.

During the drying process, all weighing steps were conducted in <10 s, and the drying was performed until the sample weight was constant with a moisture content of 5% (w.b).

All drying experiments were realized in triplicate and the results given are an average of these

experiments. The specification of each procedure is summarized below.

Hot air convective drying was realized at a set of 40, 60, 80, 100, and 120°C in a forced convection oven (VENTICELL). With an air velocity of 3 m/s as gauged by an anemometer (Juan GM816). For microwave drying, a domestic digital microwave oven (LG Model No: MS2535GISW/00) was used. The microwave oven can operate at five different power levels 200, 400, 600, 800, and 1000 W.

In vacuum drying procedures, the flower buds were dried at temperature levels 40, 60, and 80°C under a pressure of 50 mbar in a vacuum oven (MEMMERT VO200, Germany).

Drying kinetics modeling

To describe the thin-layer drying process, laboratory-based modeling is required.

In this work, 30 equations were evaluated in Table 1.

Table 1. Thin-layer drying models applied to the flower buds of *Capparis spinosa* drying kinetic curves (Hentabli et al. 2021).

Code	Model name	Equation
M1	Newton	$MR = \exp(-Kt)$
M2	Page	$MR = \exp(-Kt^n)$
M3	Modified page	$MR = \exp[-(Kt)^n]$
M4	Otsura et al.	$MR = 1 - \exp[-(Kt)^n]$
M5	Henderson and pabis	$MR = a \exp(-Kt)$
M6	Modified Henderson and pabis 1	$MR = a \exp(-K_0t) + b \exp(-K_1t) + c \exp(-K_2t)$
M7	Modified Henderson and pabis 2	$MR = a \exp(-kt^n) + b \exp(-gt) + c \exp(-ht)$
M8	Logarithmic	$MR = a \exp(-Kt) + c$
M9	Two term	$MR = a \exp(-K_0t) + b \exp(-K_1t)$
M10	Modified two term 1	$MR = a \exp(-K_0t) + a \exp(-K_1t)$
M11	Modified two term 2	$MR = a \exp(-K_0t) + (1-a)\exp(-K_1t)$
M12	Two term Exponential	$MR = a \exp(-kt) + (1-a)\exp(-kat)$
M13	Verma et al.	$MR = a \exp(-K_0t) + (1-a)\exp(-gt)$
M14	Modified Midilli 1	$MR = \exp(-Kt^n) + bt$
M15	Modified Midilli 2	$MR = \exp(-Kt) + bt$
M16	Modified Midilli 3	$MR = a \exp(-Kt) + bt$
M17	Midilli and kukuk	$MR = a \exp(-kt)^n + bt$
M18	Wang and singh	$MR = 1 + at + bt^2$
M19	Wang et al. one term	$MR = a \exp(bkt) + (1-a)$
M20	Wang et al. two term	$MR = (1-a)\exp(bkt) + a \exp(ckt)$
M21	Vega-galvez et al.	$MR = (a + bt)^2$
M22	Jena das	$MR = a \exp(-kt + b\sqrt{t}) + c$
M23	Diffusion approach	$MR = a \exp(-kt) + (1-a)\exp(-kbt)$
M24	Hii and al	$MR = a \exp(-kt)^n + c \exp(-gt^n)$
M25	Weibull distribution 1	$MR = a - b \exp[-(kt)^n]$
M26	Weibull distribution 2	$MR = \exp[-(t/a)^n]$
M27	Parabolic	$MR = a + bt + ct^2$
M28	Logistic	$MR = b/(1 + a \exp(kt))$
M29	Sledz et al.	$MR = b \exp(-kt)/(1 + a \exp(k_1t))$
M30	Demir et al.	$MR = a \exp(-kt)^n + b$

k, k_0, k_1, k_2 : drying coefficients (1/min); a, b, c, g, h : coefficients of the equations; n : exponent; t : time (min).

To compute the moisture ratio (MR) and drying rate (DR), the following formulae were applied.

$$MR = \frac{MC_t - M_e}{MC_0 - M_e} \quad (1)$$

Where MR stands for the moisture ratio, M_e is the equilibrium moisture content, M_t is the moisture content at a certain time (kg/kg db), and M_0 is the initial moisture content. It is possible to consider the equilibrium moisture content as being zero (Ovando-Medina 2023).

$$\text{Drying rate}(DR) = \frac{M_{t+dt} - M_t}{dt} \quad (2)$$

where M_t and M_{t+dt} referred to the moisture content at t and moisture content at $t + dt$ (kg/kg db), respectively, and t is drying time (min).

Heuristic techniques are widely sought after and employed by mathematicians to produce speedy and generally precise practical solutions for a specific optimization problem to improve the accuracy of traditional approaches. The dragonfly swarm optimization technique connected with the Marquardt Lavenberg nonlinear least squares algorithm (DA-nlinfit) is used in this work to achieve optimal solutions for equation parameters. This procedure's flowchart is depicted in Figure 1.

To assess the quality of the fit, the determination of coefficient (R^2), adjusted (R^2), root mean square error (RMSE), and the reduced chi-square

(x^2) were determined.

$$R^2 = 1 - \frac{\sum_{i=1}^N (MR_{exp,i} - MR_{pre,i})^2}{\sum_{i=1}^N (MR_{exp,i} - \overline{MR}_{pred,i})^2} \quad (3)$$

$$x^2 = \frac{\sum_{i=1}^N (MR_{exp,i} - MR_{pre,i})^2}{N - z} \quad (4)$$

$$RMSE = \left[\frac{\sum_{i=1}^N (MR_{exp,i} - MR_{pre,i})^2}{N} \right]^{1/2} \quad (5)$$

where $MR_{exp,i}$, $MR_{pre,i}$, N , and z are the experimental moisture ratio, the predicted moisture ratio, the data values, and the constants in the model, respectively.

Dragonfly algorithm nonlinear regression (DA-nlinfit)

Beni and Wang proposed swarm intelligence (SI) as a study subject in 1989. The major goal of this field is to comprehend the various interactions between individual living beings, which will lead to the formation of social intelligence. As a result, SI attempts to duplicate and execute collective and social intelligence characteristics exhibited in complete populations by defining rules that control interactions among selected individuals of the community. Tharwat and colleagues provided an overview of the fundamental concepts of dragonfly swarm optimization (Rahman et al. 2023).

To study experimental curves the methodology of curve fitting is usually used. It involves creating a curve with mathematical functions and fine-tuning the parameters associated with these functions to make it more closely correspond with the seen or measured curve. This process of fine-tuning the parameters is often referred to as parameter adjustment. The starting values of model coefficients are essential in the MATLAB "nlinfit" function for the least-squares approach (Hentabli et al. 2021).

The careful selection of these initial values significantly influences the speed and efficiency of the technique toward reaching a solution. In this study, adjustments of coefficients for established models from the literature were conducted using dragonfly algorithms to derive initial parameter estimates. To prevent convergence to local minima, the optimization using the dragonfly

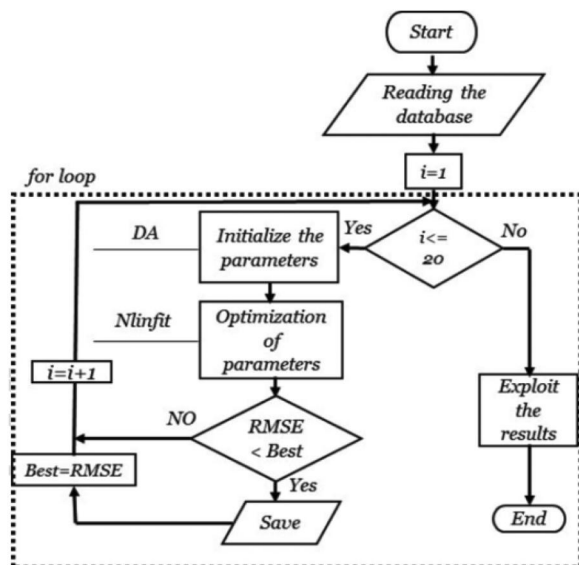


Figure 1. Flowchart of the dragonfly swarm optimization approach (Hentabli et al. 2021).

algorithm was iterated 20 times with a group of 30 dragonflies. The collection of model parameters resulting in the best fit was preserved and utilized as the initial approximation in the least-squares fitting *via* the “nlinfit” MATLAB function, employing the Levenberg-Marquardt algorithm as the computational option. In both instances, the Root Mean Square Error (RMSE) served as the objective function to minimize. Figure 1 provides an overview illustrating the sequential steps of the proposed method.

Mirjalili et al. summarized the key principles underlying swarm behavior as follows (Rahman et al. 2023).

Separation principle

The persistent avoidance of collisions by members of a population is described by this principle. The associated mathematical expression is provided by

$$S_i = - \sum_{i=1}^n (x - x_i) \quad (6)$$

In this representation, x represents the current solution's position, x_i denotes the position of individual i within the neighborhood, and n signifies the total number of members in the neighborhood.

Cohesion principle

Encapsulates the inclination of individuals to gravitate toward the central mass point of their neighborhood. Its mathematical expression is depicted as:

$$C_i = \frac{\sum_{i=1}^n x_i}{n} - x \quad (7)$$

Alignment principle

Embodies the synchronization of velocity among members of a swarm, such as dragonflies, within the same group. Its formulaic representation is:

$$A_i = \frac{\sum_{i=1}^n V_i}{n} \quad (8)$$

where V_i is the velocity of neighborhood individual i .

The flow of dragonflies in the direction of food sources can be mathematically described

$$F_i = x^+ + x \quad (9)$$

where the food's location is indicated by x^+ . Their departure from potential dangers or scavengers is described as

$$E_i = x^- + x \quad (10)$$

With, the enemy's position is x^- , A dragonfly's localization, or coordinate, is its present position x_t plus a step Δx_{t+1} . This is the total of its position. This is expressed in formal terms as follows:

$$x_{t+1} = x_t + \Delta x_{t+1} \quad (11)$$

It is possible to define the localization/coordinate of a dragonfly as follows: $x_{t+1} = x_t + \Delta x_{t+1}$, where t is the current iteration and Δx_{t+1} is found using the following equation:

$$\Delta x_{t+1} = sS_i + aA_i + cC_i + fF_i + eE_i + \omega\Delta x_i \quad (12)$$

In this instance, S_i stands for separation, and s is the separation weight; c is its weight; A_i for x_i alignment; a is its alignment weight; C_i for x_i cohesion; F_i for food attraction, and f is the food parameter; E_i for enemy distraction, e is its factor, and ω for inertia weight (Rahman et al. 2023).

The effective moisture diffusivity (D_{eff})

Although there are “constant” and “falling” rate drying periods, the former is seldom seen when drying foodstuff. The effective moisture diffusivity may be used to indicate the transport of water from the substance to the surrounding during the falling phases. According to Chen et al. (2020), this is a crucial kinetics parameter that can be calculated using Fick's second law (Equation 13) under the assumptions of uniform initial moisture distribution, negligible external resistance, constant diffusivity, constant temperature, and negligible shrinkage (Kumar A et al. 2022). Additionally, the capers shape was considered as a sphere to simplify the calculations.

$$MR = \frac{MC_t - M_e}{MC_0 - M_e} = \frac{6}{\pi^2} \sum_{n=1}^{\infty} \frac{1}{n^2} \exp\left(-n^2 \pi^2 \frac{D_{eff} t}{r_0^2}\right) \quad (13)$$

t is the drying time, D_{eff} is the effective moisture diffusion, and r_0 is the radius of the sphere (0.5 mm, measured using a Vernier caliper). MR is the moisture ratio, MC_t is the moisture content

at any time (kg water/kg dry solid), MC_0 is the initial moisture content (kg water/kg dry solid), and M_e is the equilibrium moisture content of the sample (kg water/kg dry solid).

Only the first term in the series is important for extended drying times, hence the answer is:

$$MR = \frac{6}{\pi^2} \exp\left(-\pi^2 \frac{D_{eff} t}{r_0^2}\right) \quad (14)$$

Equation (14) can be written as:

$$\ln(MR) = \ln\left(\frac{6}{\pi^2}\right) - \left(\pi^2 \frac{D_{eff} t}{r_0^2}\right) \quad (15)$$

To calculate the effective diffusivity, experimental drying data are plotted in terms of $\ln(MR)$ vs. time (s) (Kumar et al. 2022), from Equation (15). When $\ln(MR)$ vs. drying time is plotted, a straight line is produced with diffusivity as the slope.

$$slope = -\left(\frac{\pi^2 D_{eff}}{r_0^2}\right) \quad (16)$$

Activation energy

The Arrhenius type equation (Equation 17) may be used to estimate the activation energy that explains the link between the diffusivities and the conditions of drying.

$$D_{eff} = D_0 \exp\left(-\frac{E_a}{RT}\right) \quad (17)$$

Where T is the absolute temperature of the air (K), E_a is the activation energy of the moisture diffusion (kJ/mol), D_0 is the pre-exponential component of the Arrhenius equation (m^2s^{-1}), and R is the gas constant (8.3143 kJ/(kmol K)).

Since temperature is not constant during microwave drying, the activation energy was calculated based on a modified Arrhenius equation (18) (Zheng et al. 2021).

$$D_{eff} = D_0 \exp\left(-\frac{E_a m}{p}\right) \quad (18)$$

P is the microwave power (W), D_0 is the pre-exponential factor (m^2s^{-1}), E_a is the activation energy (W g^{-1}), and m is the mass of the raw sample (g).

The determination of the diffusion coefficient and activation energy parameters can be done by

solving an optimization problem. This method has the ability to capture nonlinear interactions between variables and provide advantages like accuracy (Hentabli et al. 2021). However, we chose to use linearization methods for parameter estimation due to the drying model's complexity, the availability of experimental data, and computational concerns. These techniques balance practicality and accuracy in our parameter estimate procedure, offering simplicity and computational efficiency.

Determination of energy efficiencies of drying systems

Information about energy efficiencies could be very helpful for process design and optimization to achieve minimum energy consumption. The literature reports several measures, including energy utilization and consumption, specific heat consumption, among others, to evaluate the energy efficiencies of a specific drying system (Bhardwaj et al. 2021). For this purpose, an energy measuring electrical device (HiDANCE AC power meter 220v) was used to determine the total energy consumption of the drying treatments. Then, applying Equations (19) and (20), the specific energy consumption (SEC), and moisture extraction rate (MER) were computed (Baysan et al. 2022).

$$MER = \frac{(kg) \text{moisture removed}}{(h) \text{drying time}} \quad (19)$$

$$SEC = \frac{\text{total energy required for drying}(KWh \text{ kWh})}{\text{moisture removed}(kg)} \quad (20)$$

Quality characteristics

Preparation of sample extracts and determination of total phenolic and flavonoids content

The extract used to determine total phenolic content, total flavonoid content, and antioxidant capacities using DPPH, ABTS, and FRAP was prepared as follows. Briefly, the dried buds were grinded into a fine powder ($<250 \mu m$), and a mass of 0.25 g was extracted at $37^\circ C$ in a shaking water-bath (NÜVE Bath, NB20) with 10 ml of 80% methanol for 3h. The extract was then

centrifuged at 3500 rpm for 10 min (SIGMA model 3-16L Germany) and the supernatant was stored at 4 °C until used. Three replicates were performed for each experiment.

Folin-ciocalteu method was applied according to the protocol of Hefied et al. (2023). Gallic acid was used to construct the standard curve and the results were expressed as mg (GAE/g DW).

The protocol described by Kebal et al. (2022) was used to determine the flavonoids content in the plant extract and to calibrate the standard curve the Quercetin was used. The results were expressed as mg QE/g DW.

Determination of antioxidant activities

By using the three assays this study covers several elements of antioxidant activity, such as reducing power, free radical scavenging, and total antioxidant capacity.

For instance, the DPPH assay is widely sought out to assess the free radical scavenging ability of antioxidants. It works by measuring the capacity of antioxidants to donate hydrogen atoms or electrons to neutralize DPPH radicals, which results in a rapid color change (Parcheta et al. 2021). The FRAP assay measures the ability of antioxidants to reduce ferric (Fe^{3+}) to ferrous (Fe^{2+}) ions, which complements the DPPH assay by providing information about the electron-donating capacity of antioxidants. This method is particularly important for understanding the potential of antioxidants to act as reducing agents (Abuelizz et al. 2020).

On the other hand, the ABTS assay measures the ability of antioxidants to scavenge the ABTS radical cation. Unlike DPPH, the ABTS assay can evaluate both hydrophilic and lipophilic antioxidants, providing a broader assessment for comparing antioxidants that may not be fully assessed by the DPPH or FRAP assays alone (George et al. 2022).

The extracts were evaporated under reduced pressure and then freeze-dried. The same solvent was used to reconstitute and dilute the extracts to different concentrations before carrying-out the radical scavenging assays.

IC₅₀ was calculated using a linear regression curve from a graph in which antioxidant capacity was plotted vs. various concentrations of extract.

DPPH assay. Extracts (1 mL) were reacted with 1 mL of a 0.135 mM DPPH solution in methanol. The mixture was vortexed (vortex mixer, nahita 220–240 V-51 Hz) and was left to stand for 30 min at room temperature in the dark. Reading was obtained with UV/Vis spectrophotometer (Optizen pop, Korea) at 517 nm (El Guezane et al. 2020). The results were expressed as IC₅₀ of mg/ml of lyophilized extract. Antioxidant capacity was expressed using the equation:

$$AA\% = \left[\frac{(Abs_{control} - Abs_{sample})}{Abs_{control}} \right] \times 100 \quad (21)$$

Where $Abs_{control}$ = absorbance of DPPH solution + methanol, Abs_{sample} = absorbance of DPPH solution + extracts.

ABTS assay. The following procedure was employed to determine the ABTS free scavenging capacity (Moussa et al. 2022). In brief, ABTS⁺ radical cation was created by incubating 7 mM ABTS and 2.45 mM potassium persulfate at room temperature in the dark for 12–16 h. The ABTS⁺ solution was then diluted with ethanol to a final absorbance of 0.700 ± 0.04 using a UV/Vis spectrophotometer (Optizen pop, Korea) at 734 nm. Seventy-five microliters of different concentrations of the reconstituted extracts were mixed with 1425 μL of diluted ABTS solution. The antioxidant capacity (%) was scanned after 6 min of incubation at 734 nm. The ABTS scavenging ability of caper buds was calculated following the above formula (Equation 21).

FRAP assay. The reducing power was evaluated according to the protocol of Hammi et al. (2022). Briefly, 625 μL of sodium phosphate buffer (0.2 M, pH 6.6) were mixed with 250 μL of various concentrations of the reconstituted extracts and 625 μL of $\text{K}_3\text{Fe}(\text{CN})_6$ (1%, w/v). The mixtures were allowed to stand for 20 min at 50 °C. After cooling, 625 μL of trichloroacetic acid (TCA, 10%, w/v) was added to the reaction, and the mixtures were centrifuged at $2000 \times g$ for 10 min (SIGMA model 3-16L Germany). Next, the supernatant was combined with 625 μL of distilled water and 125 μL of 1% (w/v) FeCl_3 and incubated for 10 min. The absorbance of the solutions was measured against a blank using a UV/Vis

spectrophotometer (Optizen pop, Korea). The findings were presented in terms of EC50.

Color evaluation

The color of the dried capers was estimated in terms of CIE-Lab space coordinates with a colorimeter (Konica Minolta CM 2500d). The color data were expressed as L^* (represent the lightness index), a^* (redness/greenness), and b^* (yellowness/blueness).

Furthermore, total color differences (ΔE) were calculated using Equation (22). three replicates were tested for each experiment and the average values of the color coordinates were then obtained

$$\Delta E = \sqrt{(L_0^* - L^*)^2 + (a_0^* - a^*)^2 + (b_0^* - b^*)^2} \quad (22)$$

where L_0^* , a_0^* , b_0^* represent the coordinates of fresh capers, which were treated as control.

Statistical analysis

A one-way analysis of variance was obtained with IBM SPSS statistics 26 for Windows program to look for statistically significant differences ($p < 0.05$) using Tukey's multiple range test. The values were reported as averages with \pm standard deviations (STD).

Results and discussion

Analysis of drying curves

Figure 2 depicts the caper buds drying curves during HACD, MD, and VD. As can be observed in this figure, the general drying behavior of the caper flower buds under various means revealed that along with the drying time, the moisture content declines exponentially, faster at beginning when the water content is elevated and then dropping more slowly until it eventually stops toward the last stages of drying.

The drying techniques affected greatly the drying time, the comparison among the different drying treatments revealed that the dehydrating durations required to attain the equilibrium moisture content in hot-air convection was the longest with durations varying between 120 and 1320 min at air temperature ranging from 40 to

120 °C, followed by vacuum drying at 40, 60, and 80 °C which lasted for 653, 515, and 405 min, respectively. Whereas the process duration in the microwave was considerably small (no more than 45 min).

These results could be ascribed to the mechanisms underlying water removal phenomena. Indeed, in HACD, Convection is responsible for transferring heat to the product's surface. The remaining water diffuses to the surface through heat conduction after originally being forced off the surface. Due to the buds poor thermal conductivity, it frequently takes a long time to warm the total mass of the buds to evaporation temperature. Besides, because the outer layer is affected by drying first, the product surface dries out and its permeability declines (the process of hardening). According to Joardder and Karim (2022) and Depiver and Mallik (2023), this hardened layer creates a barrier against moisture dispersion on the product surface and extends the time it takes for moisture to be eliminated from the material.

While in vacuum drying, heat is generally passed on to samples by conduction which can be a major drawback because conduction will only take place through contact points. Nevertheless, vacuum causes the air and water vapor in the sample to expand and puff up, giving the sample a large area-to-volume ratio that improves heat and mass transmission (Shirkole et al. 2023).

Meanwhile, microwave heating is volumetric, no thermal heat flux is implicated. Microwaves penetrate the sample and create an electromagnetic field that regulates the orientation of polar molecules (water), and since the polarity of the microwave field is always changing. To adapt to this frequently shifting polarity, water turns. Such molecule spinning generates heat as a result of friction with the surroundings. Moisture diffuses outside due to heat produced inside the product (Jin et al. 2020). Because caper buds have a high moisture content, using microwave power to dry them significantly enhances moisture dispersion and shortens drying time.

Experimental results point out that the drying kinetics of the buds were significantly influenced by both temperature (in CD and VD) and

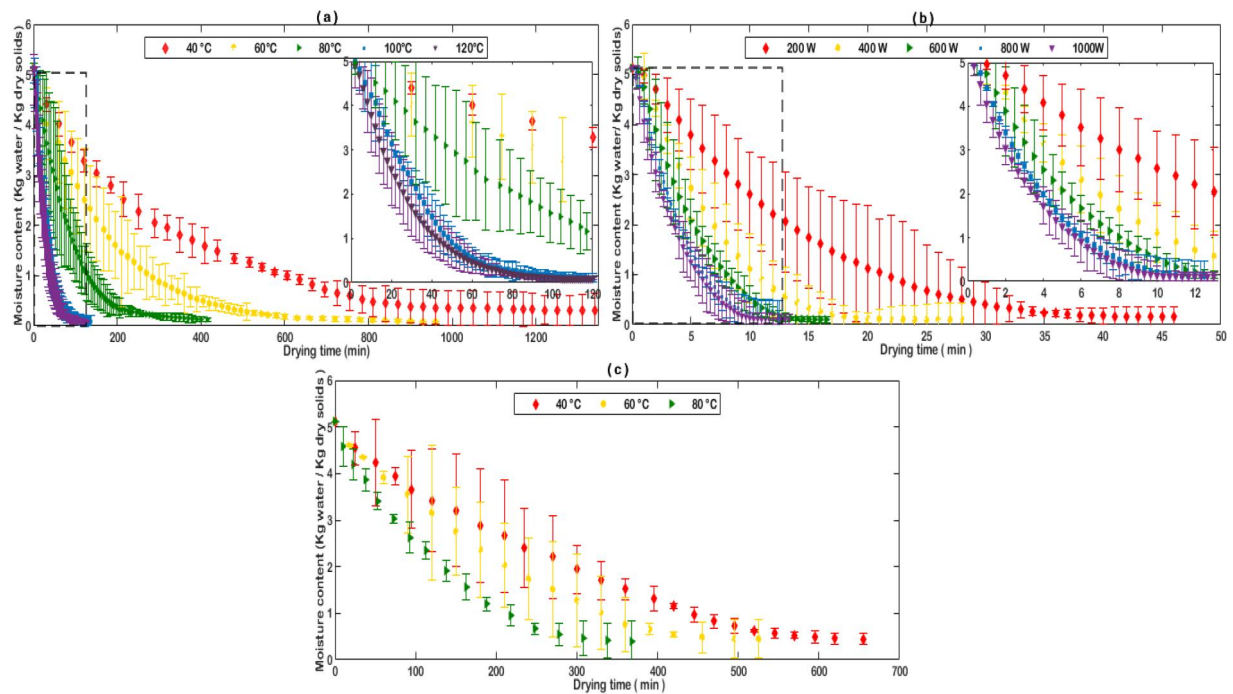


Figure 2. Moisture content kinetics of *Capparis spinosa* buds during hot-air convective drying (a), microwave drying (b), and vacuum drying (c).

microwave power input. Indeed, higher drying temperature/microwave power shortens the drying time by accelerating the drying operation. For instance, when the temperature was increased from 40 to 120 °C in HACD, the drying time needed to reach equilibrium moisture content was decreased by almost 10 times, and by three times when the microwave power level went from 200 to 1000 W and also up to three times in vacuum drying when the temperature went from 40 to 80 °C.

This result is in accordance with other papers (Abderrahim et al. 2022; Guemouni et al. 2022; Mouhoubi et al. 2022).

Analysis of drying rate

The variations of the drying rate vs. the moisture content of caper buds undergoing different drying operations are presented in Figure 3. In HACD and VD shown in Figures 3(a,c) indicated that the overall drying treatment occurred in the falling rate period. This drying behavior is very common in the thin-layer dehydration of biological samples.

The short drying duration was responsible for the brief acceleration period that was seen at the

start of HACD at high temperatures (100 and 120 °C).

The DR increased with an increase in temperature, which may be due to the enhanced heat transfer capacity between the product and the air at high temperatures. Thus facilitating the evaporation of water from it (Jmai et al. 2023).

Whilst, in microwave drying (Figure 3(b)), for all values of process variable tested, DR curves presented two stages: a rapid warming up period which was barely visible then a falling rate period where the water extraction was fast at the beginning because of the elevated amount of moisture in the sample, which led to absorb more microwave power and caused water to diffuse quickly generating high drying rates. As time goes by, a significant decrease in the drying rate was noted, which could be attributed to the low moisture content. This is in line with other works (Kipcak and Doymaz 2020; Sun et al. 2021; Yilmaz et al. 2021; Handayani et al. 2022).

Using multiple regression analyses, the drying rates along with the corresponding moisture content (MC) were plotted. The related equations and respective R^2 values are displayed in Table 2 (Supplementary Data).

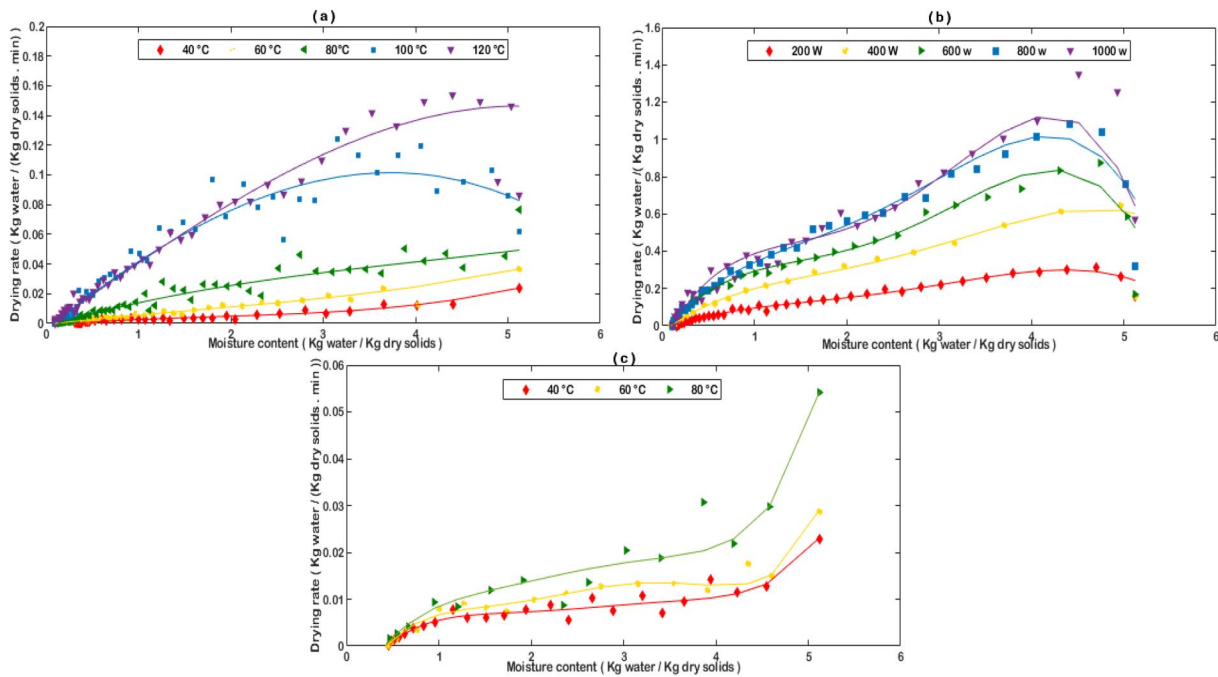


Figure 3. Drying rates vs. moisture content of *Capparis spinosa* buds during hot-air convective drying (a), microwave drying (b), and vacuum drying (c).

Mathematical modeling of drying curves

The dimensionless moisture ratio was calculated according to Equation (1) to be used for fitting the widely known thin layer models resumed in Table 1.

The suitability of each model was assessed according to the coefficients of correlation (r), adjusted (R^2), reduced chi-squared (χ^2), and RMSE values. The details of the statistical analysis are summarized in Table 1 (Supplementary Data).

The proper model illustrating the drying behavior was chosen taking into account the highest R^2 and adjusted (R^2) values, the lowest RMSE, and χ^2 values.

Among the 30 models, Jena Das model (M22) was the most accurate in predicting both the hot-air convective drying curves and the vacuum drying curves of caper buds with $0.9970 \leq R^2 \leq 0.9998$, $0.9974 \leq R^2 \leq 0.9996$, $0.0000231 \leq \chi^2 \leq 0.000255$, $0.0000494 \leq \chi^2 \leq 0.000246$, and $0.004773 \leq RMSE \leq 0.0155$, $0.007018 \leq RMSE \leq 0.01569$, respectively. This is corroborated by similar studies (Kusuma, Diwiyanto, et al. 2023; Kusuma, Sembiring, et al. 2023; Külcü et al. 2024).

As for the microwave drying process, modified Midilli 1 (M14) had the highest scores with R^2

values in the range of 0.9988 and 0.9996, χ^2 between 0.0000356 and 0.000126 and $RMSE \leq 0.0107$. This aligns with previous research (Şimşek et al. 2021; Küçük et al. 2022; Köse et al. 2024).

The experimental moisture ratio along with the predicted moisture ratio are plotted in Figure 4. It can be observed from this figure that the lines representing the chosen models in each drying treatment and condition are accurately passing through the experimental data points thus proving the models accuracy in capturing the drying properties of *Capparis spinosa* under experimental conditions.

Effective moisture diffusivity (D_{eff})

The effective moisture diffusivity was calculated using the slopes technique from Equation (16). While the R^2 values from Table 2 were obtained through linear regression of $(\ln(MR))$ data plotted against drying time.

The results are presented in Table 2. The D_{eff} values found in this study showed a variation ranging from $1.46e^{-10}$ to $21.9e^{-10} m^2s^{-1}$, in the range of $51.1e^{-10}$ and $204e^{-10} m^2s^{-1}$, and between $2.56e^{-10}$ and $3.65e^{-10} m^2s^{-1}$ for HACD, MD, and VD, respectively.

Table 2. The effective moisture diffusivity, activation energy, and the goodness of fit of different drying methods and conditions.

Drying methods	Drying conditions	Effective moisture diffusivity * e^{-10} (m^2s^{-1})	R^2	R^2 -adjusted	RMSE	x^2	Activation energy
Convective drying (°C)	40	1.46	0.9584	0.957	0.188	0.062	37.917 kJ/mol
	60	2.56	0.9514	0.950	0.261	6.424	
	80	7.30	0.9653	0.965	0.226	5.700	
	100	18.3	0.9742	0.974	0.219	7.464	
	120	21.9	0.9828	0.982	0.191	8.807	
Microwave drying (W)	200	51.1	0.9911	0.991	0.112	4.842	11.963 W/g
	400	102	0.9636	0.962	0.281	7.470	
	600	168	0.981	0.980	0.194	5.722	
	800	201	0.9927	0.993	0.109	4.978	
	1000	204	0.9776	0.977	0.205	6.298	
Vacuum drying (°C)	40	2.56	0.9873	0.987	0.094	2.168	8.256 kJ/mol
	60	3.29	0.9878	0.987	0.098	2.209	
	80	3.65	0.9912	0.991	0.088	2.290	

R^2 : regression coefficient; Radj: adjusted R^2 ; RMSE: root mean square error between experimental and predicted data; x^2 : chi-square.

These D_{eff} values fall within the widespread range of diffusivities of food samples which is 10^{-8} to $10^{-12} m^2 s^{-1}$ (Abderrahim et al. 2022).

The diffusion coefficient of the HACD, VD, and MD process, increased with increasing temperature or microwave power. The same trend was noted in microwave drying where the increase of the diffusivities was observed when the power level of the microwave was increased it may be explained in this case by the fact that high microwave power generates more energy to be absorbed by the water molecules (Abderrahim et al. 2022).

It is interesting to note that among the three drying treatments. MD yields the highest D_{eff} rates with a maximum value of $2.04 e^{-8} m^2 s^{-1}$ achieved at 1000 W.

When comparing the other drying processes at the same respective temperatures, VD was second best (except for drying at 80 °C where HAD prevailed) followed by HACD.

The results of this study parallels conclusions from other studies (Hentabli et al. 2021; Guemouni et al. 2022; Mouhoubi et al. 2022).

Activation energy (E_a)

In this work, we attempted to estimate the activation energy of HACD, VD, and MD which describe the ability of the system to remove water.

The slopes of lines were used to determine the activation energies and were found 37.917 kJ/mol, 11.963 W/g, and 8.256 kJ/mol for hot air, microwave, and vacuum drying.

The activation energy for HACD falls within the general range determined for fruits and vegetables which is between 12.7 and 110 kJ/mol (Abderrahim et al. 2022).

In microwave drying procedure, it was quite close to those reported by other researchers 7.96 W/g for banana samples (Jha et al. 2021), 10.026 W/g for white cabbage (Luka et al. 2023), 15.03 W/g for apple (Rasooli Sharabiani et al. 2021).

On the other hand, for VD its activation energy was lower than the custom values of fruits and vegetables defined above (ranging between 12.7 and 110 kJ/mol).

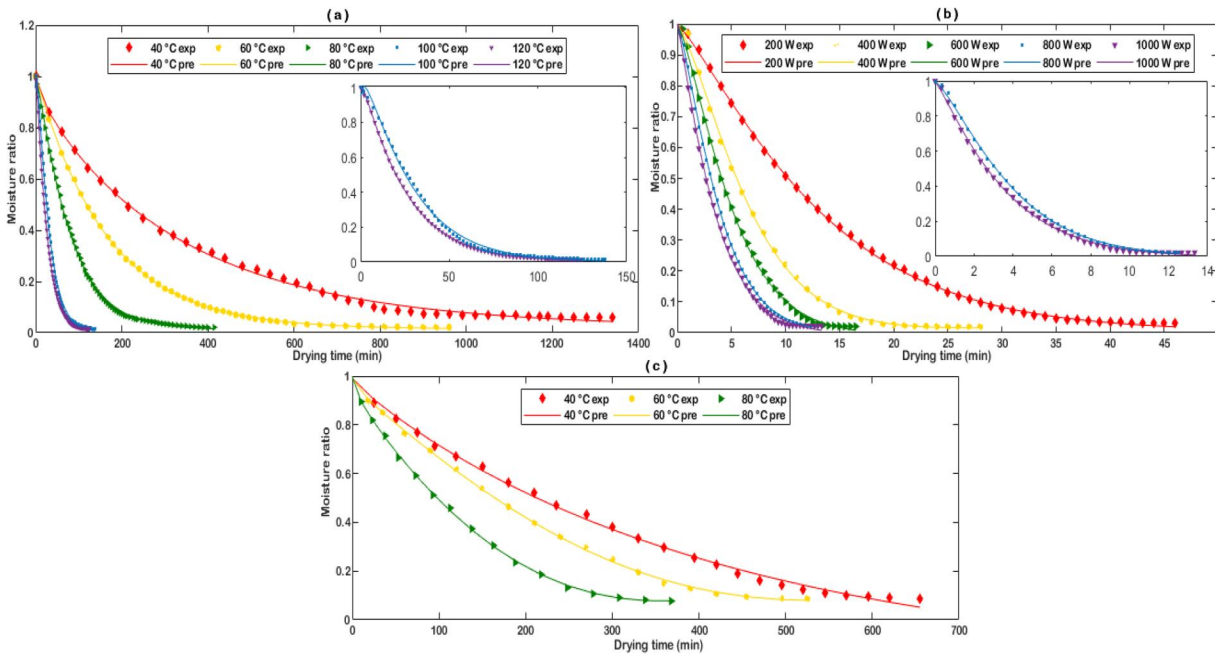


Figure 4. Experimental and predicted moisture ratio values for hot-air convective (a), microwave (b), and vacuum (c) drying treatments of *Capparis spinosa* buds.

Table 3. The results of energy efficiency of different drying methods and conditions.

Drying methods	Drying conditions	MER (kg/h)* 10^{-2}	SEC (kWh/kg)
Convective drying ($^{\circ}$ C)	40	0.11 ± 0.004^e	40.852 ± 1.337^d
	60	0.16 ± 0.008^e	28.772 ± 1.324^{de}
	80	0.37 ± 0.012^e	15.268 ± 0.377^e
	100	1.08 ± 0.004^e	11.167 ± 0.031^e
	120	1.24 ± 0.052^e	15.2847 ± 0.142^e
Microwave drying (W)	200	3.24 ± 0.068^d	16.6229 ± 0.346^e
	400	6.55 ± 0.51^c	10.8617 ± 0.866^e
	600	9.13 ± 0.177^b	10.4957 ± 0.206^e
	800	11.98 ± 0.405^a	10.6887 ± 0.354^e
	1000	12.16 ± 1.494^a	13.1559 ± 1.535^e
Vacuum drying ($^{\circ}$ C)	40	0.21 ± 0.002^e	82.663 ± 0.771^b
	60	0.27 ± 0.009^e	65.155 ± 2.177^{bc}
	80	0.34 ± 0.08^e	50.667 ± 1.268^{cd}

Values are mean \pm 95% confidence interval.

Values with different letters (a–e) were significantly different (Tukey, $p < 0.05$).

Energy efficiencies of drying systems

A comparison of energy efficiencies for various dehydration systems is illustrated in Table 3.

MER values varied between 0.0011 and 0.0123 (kg/h) for hot-air convective drying, from 0.0324 to 0.1216 (kg/h) for MD, and from 0.0021 to 0.0034 (kg/h) for VD.

Results indicated that with increasing temperature or power level, the MER values increased. The minimum moisture extraction rate (0.0011 kg/h) and maximum MER (0.1216 kg/h) are obtained with hot-air convective drying at 40° C and a microwave power level of 1000 W, respectively.

The best results were achieved by microwave followed by the other processes with no significant difference between them, this confirms that drying with microwave is very effective compared to the other operations.

The opposite trend was noted, in terms of the SEC values. Indeed, despite the slight increase in the values of SEC at the highest temperature (120° C) and microwave power level (1000 W), lower temperature/microwave power was more energy-intensive compared to a higher temperature or power level, this may be explained by the fact that SEC is highly correlated with drying time and as high temperatures/power reduces the

drying times, it consequently makes the process less energy consuming.

These results resemble those of others (Kaveh et al. 2021; Mouhoubi et al. 2022), Kaveh et al. who stated that the SEC for convective drying decreases with increasing air temperature.

Effect of drying on the bioactive compounds

Table 4 displays the total polyphenolic content and total flavonoid amount in fresh and dried caper buds. The TPC and TFC present in the fresh *Capparis spinosa* flower-buds were determined to be 36.20 ± 1.46 mg GAE/g DW and 11.58 ± 0.17 mg QE/g DW, respectively.

The phenolic content obtained in this study was similar to those ranging between 1843.71 and 3870 GAE mg/100 g DW found in another paper (Shahrajabian et al. 2021). The flavonoids content however was lower (21.35 ± 2.20 and 15.41 ± 0.88 mg QE/g DW) than those reported in other studies (Tayiroğlu and İncedayı 2021). These observed differences may be resulted from various factors, such as harvest regions, product maturity, the type of solvents, and processing factors.

The amount of TPC and TFC in the dried caper buds displayed the same trend for the different drying treatments. For instance, a remarkable reduction had occurred after the drying treatments. The loss rate of TPC and TFC in HACD was higher than the other drying methods particularly at 40°C (2.13%), possibly due to the long drying times and the elevated temperature. Previous study reported similar findings (Xu et al. 2020).

Followed by MD (from 1.32 to 1.63% for TPC and from 1.27 to 1.77% in TFC) then VD, where a reduction of 1.19–1.34% in TPC and 1.13–1.43% in TFC was noted.

Findings indicated that polyphenols and flavonoids are heat sensitive and that thermal exposure for long duration result in substantial thermal destruction of polyphenols and flavonoids (Ng et al. 2021). Furthermore, peroxidase and polyphenoloxidase activity during the drying process in MD and HACD might result in TPC loss. Meanwhile in vacuum drying the enzymes activities is suppressed which may explain the better recovery of the bioactive compounds

Table 4. The results of the quality characteristics of different drying methods and conditions.

Drying methods	Drying conditions	TPC (mg GAE/g DW)	TFC (mg QE/g DW)	DPPH (IC50 mg/mL)	ABTS (IC50 mg/mL)	FRAP (IC50 mg/mL)	1	a	b	ΔE
Fresh		$36.20^{ab} \pm 1.46$	$11.58^b \pm 0.17$	$0.176^{\pm} \pm 0.028$	$1.154^{\pm} \pm 0.046$	$0.096^{\pm} \pm 0.081$	$43.16^{\pm} \pm 0.13$	$-4.08^n \pm 0.04$	$10.80^{\pm} \pm 0.68$	$5.39^{\pm} \pm 0.02$
Convective drying ($^\circ\text{C}$)	40	$16.96^g \pm 2.52$	$2.85^{\pm} \pm 0.26$	$0.479^{\pm} \pm 0.026$	$13.435^{\pm} \pm 0.909$	$0.397^{\text{defi}} \pm 0.024$	$42.27^{\pm} \pm 0.15$	$-0.75^{\text{k}} \pm 0.01$	$6.65^{\text{cd}} \pm 0.02$	$6.64^{\pm} \pm 0.02$
	60	$17.22^g \pm 0.46$	$3.04^{\pm} \pm 0.13$	$0.453^{\text{ab}} \pm 0.072$	$9.168^{\pm} \pm 0.207$	$0.478^{\text{defi}} \pm 0.105$	$40.40^{\pm} \pm 0.01$	$-1.32^{\text{k}} \pm 0.02$	$5.42^{\text{f}} \pm 0.03$	$8.89^{\pm} \pm 0.01$
	80	$20.29^{\text{fig}} \pm 2.51$	$4.43^{\text{h}} \pm 0.37$	$0.410^{\text{abcde}} \pm 0.020$	$8.544^{\pm} \pm 0.687$	$0.381^{\text{fi}} \pm 0.030$	$39.06^g \pm 0.02$	$0.47^{\text{i}} \pm 0.02$	$4.35^{\text{h}} \pm 0.02$	$8.89^{\pm} \pm 0.01$
	100	$19.22^{\text{ig}} \pm 1.25$	$4.82^{\text{efi}} \pm 0.06$	$0.376^{\text{abcde}} \pm 0.004$	$8.409^{\pm} \pm 0.280$	$0.456^{\text{defi}} \pm 0.031$	$40.77^{\text{e}} \pm 0.07$	$0.82^{\text{e}} \pm 0.02$	$6.18^{\text{de}} \pm 0.02$	$7.14^{\pm} \pm 0.02$
Microwave drying (W)	120	$20.87^{\text{efig}} \pm 3.96$	$5.32^{\text{efc}} \pm 1.86$	$0.428^{\text{abc}} \pm 0.070$	$6.915^{\text{bcde}} \pm 1.037$	$0.561^{\text{cd}} \pm 0.018$	$36.84^{\pm} \pm 0.05$	$0.85^{\text{e}} \pm 0.02$	$1.50^{\text{k}} \pm 0.02$	$12.28^{\text{b}} \pm 0.02$
	200	$23.25^{\text{defig}} \pm 1.63$	$6.70^{\text{de}} \pm 0.96$	$0.326^{\text{cdef}} \pm 0.041$	$5.319^{\text{def}} \pm 0.481$	$1.021^{\pm} \pm 0.059$	$36.20^{\pm} \pm 0.03$	$0.91^{\text{d}} \pm 0.02$	$1.35^{\text{k}} \pm 0.01$	$12.75^{\pm} \pm 0.02$
	400	$27.33^{\text{cde}} \pm 3.67$	$9.09^{\pm} \pm 1.40$	$0.305^{\text{def}} \pm 0.032$	$4.975^{\text{ef}} \pm 0.058$	$0.825^{\text{b}} \pm 0.024$	$37.14^{\pm} \pm 0.05$	$1.01^{\text{c}} \pm 0.02$	$2.12^g \pm 0.02$	$11.72^{\text{c}} \pm 0.04$
	600	$24.46^{\text{cde}} \pm 4.42$	$8.65^{\text{cd}} \pm 0.47$	$0.298^{\text{ef}} \pm 0.007$	$6.153^{\text{cdef}} \pm 2.319$	$0.652^{\text{c}} \pm 0.043$	$38.41^{\text{h}} \pm 0.04$	$1.20^{\text{b}} \pm 0.01$	$2.58^g \pm 0.02$	$10.86^{\text{d}} \pm 0.02$
Vacuum drying ($^\circ\text{C}$)	800	$25.36^{\text{cde}} \pm 2.16$	$8.20^{\text{cd}} \pm 0.54$	$0.334^{\text{cdef}} \pm 0.020$	$5.804^{\text{def}} \pm 0.585$	$0.490^{\text{def}} \pm 0.027$	$37.83^{\pm} \pm 0.03$	$0.73^{\text{f}} \pm 0.02$	$3.47^{\text{f}} \pm 0.02$	$10.26^{\text{e}} \pm 0.03$
	1000	$22.12^{\text{efig}} \pm 1.30$	$6.54^{\text{def}} \pm 0.51$	$0.350^{\text{cdef}} \pm 0.034$	$7.497^{\text{bcd}} \pm 0.664$	$0.487^{\text{def}} \pm 0.027$	$40.54^{\pm} \pm 0.04$	$1.34^{\text{a}} \pm 0.02$	$5.46^{\text{f}} \pm 0.01$	$8.04^g \pm 0.00$
	40	$26.97^{\text{cde}} \pm 0.11$	$8.07^{\text{cd}} \pm 0.36$	$0.333^{\text{cdef}} \pm 0.008$	$5.651^{\text{def}} \pm 0.271$	$0.353^{\text{f}} \pm 0.017$	$42.82^{\text{b}} \pm 0.02$	$-0.96^g \pm 0.02$	$6.95^{\text{c}} \pm 0.02$	$4.96^{\text{m}} \pm 0.02$
	60	$29.21^{\text{cd}} \pm 0.63$	$8.53^{\text{cd}} \pm 0.43$	$0.303^{\text{def}} \pm 0.011$	$4.919^{\text{ef}} \pm 0.140$	$0.438^{\text{defi}} \pm 0.009$	$41.45^{\text{d}} \pm 0.03$	$-2.02^{\pm} \pm 0.02$	$5.83^{\text{ef}} \pm 0.02$	$5.64^{\text{k}} \pm 0.01$
	80	$30.18^{\text{bc}} \pm 0.59$	$10.27^{\text{c}} \pm 0.23$	$0.249^{\text{f}} \pm 0.021$	$4.448^{\pm} \pm 0.089$	$0.517^{\text{de}} \pm 0.010$	$40.86^{\text{e}} \pm 0.02$	$0.08^{\text{h}} \pm 0.02$	$5.03^{\text{h}} \pm 0.06$	$7.47^{\text{h}} \pm 0.05$

Values are mean \pm SD.

Values with different letters (a–n) were significantly different (Tukey, $p < 0.05$).

compared to the other drying treatments (Harguindeguy et al. 2021).

Effect of drying on antioxidant activity

ABTS, DPPH, and FRAP assays were used to evaluate the antioxidant activities of fresh and dried *Capparis* extracts.

The concentration of the extract needed to scavenge 50% of radicals was estimated as the IC50. The sample's antioxidant capabilities increase with decreasing IC50 values.

In regard DPPH and ABTS, the overall IC50 values showed similar tendency, where the fresh samples exhibited the highest scavenging activities (IC50 = 0.176 mg/mL in DPPH and IC50 = 1.154 in ABTS). Thermal drying methods on the other hand caused a decrease in the antioxidant activity. It indicates that during the heating process, the cellular structure disintegrates, oxidizing thermo-labile chemicals that are prone to deterioration (Kumar et al. 2022).

The lowest DPPH and ABTS radical powers were recorded in the HACD treatments (the 40 °C sample was the most effected). While the buds produced by VD method demonstrated better scavenging activities than MD. Furthermore, the DPPH showed high correlation with TPC ($R^2 = 0.9116$) and TFC ($R^2 = 0.9447$). Similarly, ABTS values were highly correlated with TPC ($R^2 = 0.852$) and TFC ($R^2 = 0.8616$). This may indicate that these phenolic compounds (TPC and TFC) are responsible for the scavenging activities available in the samples. Similar types of findings were also reported by (Chumroenphat et al. 2021; Kumar D et al. 2022).

In FRAP assay, a different trend was noted, fresh samples displayed higher scavenging activities than the freeze-dried samples, followed by VD 40 °C > HACD 80 °C > HACD 40 °C > VD 60 °C > HACD 100 °C > HACD 60 °C > MD 1000 W > MD 800 W > VD 80 °C > HCD 120 °C > MD 600 W > MD 400 W > MD 200 W, respectively. Moreover, the FRAP reducing ability presented weak correlation with TPC ($R^2 = 0.179$) and TFC ($R^2 = 0.083$).

These results indicated that low pressure treatment VD were more efficient to preserve the antioxidant activity of *Capparis* buds, followed by MD then HACD.

Our results are in agreement with other works (Farahmandfar et al. 2020; Turkiewicz et al. 2020).

Effect of the drying on color

The evaluation of color serves several key purposes: first, color is often the first characteristic noticed by consumers and can be an indicator of the overall quality and freshness of the food product. Changes in color during the drying process can reflect the extent of Maillard reactions, enzymatic browning, or pigment degradation, which are important indicators of the nutritional and sensory qualities of the food.

Second, even slight changes in color can influence a consumer's perception of the product's quality and desirability, making color evaluation crucial for marketability.

Lastly, in some cases, dried food products or their extracts are used as natural colorants in other food applications. For example, maintaining or enhancing the color of dried *Capparis spinosa* buds could make them valuable as a natural green colorant, adding esthetic and functional value to various food products (Pathare et al. 2013).

Fresh and dried capers Hunter L^* , a^* , b^* coordinates are shown in Table 4. The dehydration processes remarkably influenced the color values of the flower-buds ($p < 0.05$). All the drying processes caused a decrease in the L^* value which resulted in a dark dried samples compared to the fresh ones. Negative a^* scores which speculate greenness was observed in fresh buds, VD at 40, 60 °C, and CD at 40, 60 °C. While the other drying experiments led to a positive a^* values that signify the obtention of samples with red hues at their surface. This could be attributed to the loss of green pigment associated with the high temperature (Turgay and Esen 2020).

The b^* value of the fresh sample showed a significant decrease after dehydration depending on the conditions applied. In general, the increasing temperature was associated with a reduction in the b^* values except in MD where the opposite trend was observed.

In terms of the ΔE , the lowest color difference was recorded in the VD (4.96) which indicate that this drying method was effective in

preserving the color of the fresh capers. Followed by HACD, respectively. With increasing ΔE values linked to the increasing temperature. In contrast, MD showed high color difference at the low power level.

These results demonstrated that the color of the dried capers was susceptible to high temperature and duration of thermal treatment.

Despite the scarcity of studies in the literature directly addressing capers drying, these findings align with previous research on other food items (Yildiz 2022; de Mendonça et al. 2023).

Conclusion

The drying kinetics of *Capparis* flower buds under hot-air convective, vacuum, and microwave drying techniques were examined in this study.

The results indicated that the water removal during the dehydration of caper buds occurred in the falling-rate phase.

Mathematical fitting of the drying curves showed that Jena Das model efficiently described the drying kinetics of the buds in both hot-air convective drying and vacuum drying, while modified Midilli 1 was suitable for describing microwave drying behavior of the buds, respectively.

The highest diffusivities were obtained with microwave drying. When comparing the three drying operations in terms of energy efficiencies, the results revealed that microwave drying at 1000 W was the most efficient drying method.

In regard to the quality of the dried caper, convective drying exhibited the most pronounced impact on the degradation of total phenolics and flavonoids, especially notable at 40 °C, where the loss reached 2.13%. This heightened loss can likely be attributed to the extended drying durations and the higher operating temperature characteristic of the HACD process. Subsequent to HACD, Microwave Drying (MD) displayed intermediate loss rates ranging from 1.32 to 1.63% for the TPC and from 1.27 to 1.77% for the TFC. Conversely, Vacuum Drying (VD) demonstrated comparatively lower loss rates, with reductions ranging between 1.19 to 1.34% for TPC and 1.13 to 1.43% for TFC. A similar trend was observed for DPPH and ABTS, which was demonstrated

by the high correlation between these radical scavenging activities and the phenolic and flavonoid content, suggesting that these phenolic compounds (TPC and TFC) are primarily responsible for the scavenging activities present in the samples. Regarding the color of the buds, the lowest color difference was recorded in VD at 40 °C (4.96), indicating that this drying method effectively preserved the color of the fresh capers. This was followed by HACD and MD, respectively.

It can thus be concluded that vacuum drying at 80 °C has a minimal impact on the quality of capers, whereas microwave drying at 1000 W is more efficient in terms of drying performance.

Disclosure statement

No potential conflict of interest was reported by the author(s).

References

- Abderrahim KA, Remini H, Dahmoune F, Mouhoubi K, Berkani F, Abbou A, Aoun O, Dairi S, Belbahi A, Kadri N, et al. 2022. Influence of convective and microwave drying on Algerian blood orange slices: drying kinetics and characteristics, modeling, and drying energetics. *J Food Process Eng.* 45(12):e14176. doi:10.1111/jfpe.14176.
- Abuelizz HA, Anouar E, Marzouk M, Taie HA, Ahudhaif A, Al-Salahi R. 2020. DFT study and radical scavenging activity of 2-phenoxy pyridotriazolo pyrimidines by DPPH, ABTS, FRAP and reducing power capacity. *Chem Pap.* 74(9):2893–2899. doi:10.1007/s11696-020-01126-0.
- Aksay O, Selli S, Kelebek H. 2021. LC-DAD-ESI-MS/MS-based assessment of the bioactive compounds in fresh and fermented caper (*Capparis spinosa*) buds and berries. *Food Chem.* 337:127959. doi:10.1016/j.foodchem.2020.127959.
- Ali LH, Abdulhadi HL, Mohammed NA. 2023. The protective effects of *Capparis spinosa* aqueous extract against methotrexate in male albino rats. *Med J Babylon.* 20(4): 886–890. doi:10.4103/MJBL.MJBL_1156_23.
- Arslan A, Soysal Y, Keskin M. 2020. Mathematical modeling, moisture diffusion and color quality in intermittent microwave drying of organic and conventional sweet red peppers. *AgriEngineering.* 2(3):393–407. doi:10.3390/agriengineering2030027.
- Assadi S, Shafiee SM, Erfani M, Akmal M. 2021. Antioxidative and antidiabetic effects of *Capparis spinosa* fruit extract on high-fat diet and low-dose streptozotocin-induced type 2 diabetic rats. *Biomed Pharmacother.* 138: 111391. doi:10.1016/j.biopha.2021.111391.
- Banwo K, Olojede AO, Adesulu-Dahunsi AT, Verma DK, Thakur M, Tripathy S, Singh S, Patel AR, Gupta AK,

- Aguilar CN, et al. 2021. Functional importance of bio-active compounds of foods with potential health benefits: a review on recent trends. *Food Biosci.* 43:101320. doi:10.1016/j.fbio.2021.101320.
- Baysan U, Koç M, Güngör A, Ertekin FK. 2022. Investigation of drying conditions to valorize 2-phase olive pomace in further processing. *Drying Technol.* 40(1):65–76. doi:10.1080/07373937.2020.1770279.
- Bechlin TR, Granella SJ, Christ D, Coelho SRM, Paz CHO. 2020. Effects of ozone application and hot-air drying on orange peel: moisture diffusion, oil yield, and antioxidant activity. *Food Bioprod Process.* 123:80–89. doi:10.1016/j.fbp.2020.06.012.
- Bhardwaj A, Kumar R, Kumar S, Goel B, Chauhan R. 2021. Energy and exergy analyses of drying medicinal herb in a novel forced convection solar dryer integrated with SHSM and PCM. *Sustain Energy Technol Assess.* 45: 101119. doi:10.1016/j.seta.2021.101119.
- Buzrul S. 2022. Reassessment of thin-layer drying models for foods: a critical short communication. *Processes.* 10(1):118. doi:10.3390/pr10010118.
- Calín-Sánchez Á, Lipan L, Cano-Lamadrid M, Kharaghani A, Masztalerz K, Carbonell-Barrachina ÁA, Figiel A. 2020. Comparison of traditional and novel drying techniques and its effect on quality of fruits, vegetables and aromatic herbs. *Foods.* 9(9):1261. doi:10.3390/foods9091261.
- Carvalho GR, Monteiro RL, Laurindo JB, Augusto PED. 2021. Microwave and microwave-vacuum drying as alternatives to convective drying in barley malt processing. *Innov Food Sci Emerg Technol.* 73:102770. doi:10.1016/j.ifset.2021.102770.
- Chen C, Venkatasamy C, Zhang W, Khir R, Upadhyaya S, Pan Z. 2020. Effective moisture diffusivity and drying simulation of walnuts under hot air. *Int J Heat Mass Transf.* 150:119283. doi:10.1016/j.ijheatmasstransfer.2019.119283.
- Chumroenphat T, Somboonwatthanakul I, Saensouk S, Siriamornpun S. 2021. Changes in curcuminoids and chemical components of turmeric (*Curcuma longa* L.) under freeze-drying and low-temperature drying methods. *Food Chem.* 339:128121. doi:10.1016/j.foodchem.2020.128121.
- Cincotta F, Merlino M, Verzera A, Gugliandolo E, Conduro C. 2022. Innovative process for dried caper (*Capparis spinosa* L.) powder production. *Foods.* 11(23): 3765. doi:10.3390/foods11233765.
- de Mendonça KS, Corrêa JLG, de Jesus Junqueira JR, de Carvalho EEN, Silveira PG, Uemura JHS. 2023. Peruvian carrot chips obtained by microwave and microwave-vacuum drying. *LWT.* 187:115346. doi:10.1016/j.lwt.2023.115346.
- Demir H, Demir H, Lončar B, Nićetin M, Pezo L, Yilmaz F. 2023. Artificial neural network and kinetic modeling of capers during dehydration and rehydration processes. *J Food Process Eng.* 46(2):e14249. doi:10.1111/jfpe.14249.
- Depiver JA, Mallik S. 2023. An empirical study on convective drying of ginger rhizomes leveraging environmental stress chambers and linear heat conduction methodology. *Agriculture.* 13(7):1322. doi:10.3390/agriculture13071322.
- El Guezane C, El Moudden H, Harhar H, Zarrouk A, Tabyaoui M. 2020. Optimization the effect of roasting conditions by central composite design (CCD) method on the antioxidant compounds of *Opuntia ficus indica* seeds from Morocco.
- Elshibani F, Alamami A, Alshalmani S, El Naili EA, Gehawe HA, Sharkasi MA, Elremali N. 2020. Estimation of phenolic content, flavonoid content, antioxidant properties and alpha-amylase inhibitory activities of *Capparis spinosa* L. *J Pharmacogn Phytochem.* 9(4):24–28.
- Farahmandfar R, Tirgarian B, Dehghan B, Nemati A. 2020. Changes in chemical composition and biological activity of essential oil from Thomson navel orange (*Citrus sinensis* L. Osbeck) peel under freezing, convective, vacuum, and microwave drying methods. *Food Sci Nutr.* 8(1):124–138. doi:10.1002/fsn3.1279.
- George J, Edwards D, Pun S, Williams D. 2022. Evaluation of antioxidant capacity (ABTS and CUPRAC) and total phenolic content (Folin-Ciocalteu) assays of selected fruit, vegetables, and spices. *Int J Food Sci.* 2022(1):2581470–2581418. doi:10.1155/2022/2581470.
- Granella SJ, Bechlin TR, Christ D. 2022. Moisture diffusion by the fractional-time model in convective drying with ultrasound-ethanol pretreatment of banana slices. *Innov Food Sci Emerg Technol.* 76:102933. doi:10.1016/j.ifset.2022.102933.
- Grimalt M, Hernández F, Legua P, Amorós A, Almansa MS. 2022. Antioxidant activity and the physicochemical composition of young caper shoots (*Capparis spinosa* L.) of different Spanish cultivars. *Sci Hortic.* 293:110646. doi:10.1016/j.scienta.2021.110646.
- Guemouni S, Mouhoubi K, Brahmi F, Dahmoune F, Belbahi A, Benyoub C, Adjeroud-Abdellatif N, Atmani K, Bakhouché H, Boulekbache-Makhlouf L, et al. 2022. Convective and microwave drying kinetics and modeling of tomato slices, energy consumption, and efficiency. *J Food Process Eng.* 45(9):e14113. doi:10.1111/jfpe.14113.
- Hammi KM, Essid R, Khadraoui N, Ksouri R, Majdoub H, Tabbene O. 2022. Antimicrobial, antioxidant and anti-leishmanial activities of *Ziziphus lotus* leaves. *Arch Microbiol.* 204(1):119. doi:10.1007/s00203-021-02733-5.
- Handayani S, Mujiarto I, Siswanto A, Ariwibowo D, Atmanto I, Mustikaningrum M. 2022. Drying kinetics of chilli under sun and microwave drying. *Mater Today Proc.* 63:S153–S158. doi:10.1016/j.matpr.2022.02.119.
- Harguindeguy M, Bobba S, Colucci D, Fissore D. 2021. Effect of vacuum freeze-drying on the antioxidant properties of eggplants (*Solanum melongena* L.). *Drying Technol.* 39(1):3–18. doi:10.1080/07373937.2019.1699834.
- Hefied F, Ahmed ZB, Yousfi M. 2023. Optimization of ultrasonic-assisted extraction of phenolic compounds and antioxidant activities from *Pistacia atlantica* Desf. galls using response surface methodology. *J Appl Res Med*

- Aromat Plants. 32:100449. doi:10.1016/j.jarmap.2022.100449.
- Hentabli M, Belhadj A-E, Benimam H, Dahmoune F, Keskes S. 2021. Vacuum drying of the terbinafine HCl powder: a kinetics study and mathematical modeling. Powder Technol. 383:220–232. doi:10.1016/j.powtec.2021.01.038.
- Horuz E, Bozkurt H, Karatas H, Maskan M. 2020. Microwave-conventional drying characteristics of red pepper: modeling, temperature profile, diffusivity and activation energy. J Agric Sci Technol. 22(2):425–437.
- Jahanbakhshi A, Kaveh M, Taghinezhad E, Rasooli Sharabiani V. 2020. Assessment of kinetics, effective moisture diffusivity, specific energy consumption, shrinkage, and color in the pistachio kernel drying process in microwave drying with ultrasonic pretreatment. J Food Process Preserv. 44(6):e14449. doi:10.1111/jfpp.14449.
- Jha P, Meghwal M, Prabhakar PK. 2021. Microwave drying of banana blossoms (*Musa acuminata*): mathematical modeling and drying energetics. J Food Process Preserv. 45(9):e15717. doi:10.1111/jfpp.15717.
- Jin W, Zhang M, Shi W, Mujumdar AS. 2020. Recent developments in high-quality herbs and spices drying of herbs, spices and medicinal plants: processing, health benefits and safety.
- Jmai S, Ben Slimane N, Masouddi S, Guiza S, Mohamed B. 2023. Experimental and modeling of tomato slices sorption isotherms and thin layer drying kinetics for a solar drying plant design. Iran J Chem Chem Eng. 42(8):2587–2603.
- Joardder MU, Karim M. 2022. Drying kinetics and properties evolution of apple slices under convective and intermittent-MW drying. Therm Sci Eng Prog. 30:101279. doi:10.1016/j.tsep.2022.101279.
- Kant R, Kushwah A, Kumar A, Kumar M. 2023. Solar drying of peppermint leave: thermal characteristics, drying kinetics, and quality assessment. J Stored Prod Res. 100:102068. doi:10.1016/j.jspr.2022.102068.
- Kaveh M, Golpour I, Gonçalves JC, Ghafouri S, Guiné R. 2021. Determination of drying kinetics, specific energy consumption, shrinkage, and colour properties of pomegranate arils submitted to microwave and convective drying. Open Agric. 6(1):230–242. doi:10.1515/opag-2020-0209.
- Kebal L, Pokajewicz K, Djebli N, Mostefa N, Poliwoda A, Wieczorek PP. 2022. HPLC-DAD profile of phenolic compounds and *in vitro* antioxidant activity of *Ficus carica* L. fruits from two Algerian varieties. Biomed Pharmacother. 155:113738. doi:10.1016/j.biopha.2022.113738.
- Kerr WL, Varner A. 2020. Chemical and physical properties of vacuum-dried red beetroot (*Beta vulgaris*) powders compared to other drying methods. Drying Technol. 38(9):1165–1174. doi:10.1080/07373937.2019.1619573.
- Khanavi M, Ara L, Khavassi N, Hajimehdipoor H. 2020. *Caparis spinosa*: a comparative study of raw and processed fruits. J Med Plants. 1(73):91–99. doi:10.29252/jmp.1.73.91.
- Kipcak AS, Doymaz I. 2020. Mathematical modeling and drying characteristics investigation of black mulberry dried by microwave method. Int J Fruit Sci. 20(sup3):S1222–S1233. doi:10.1080/15538362.2020.1782805.
- Kittibunchakul S, Temviriyankul P, Chaikham P, Kemsawasd V. 2023. Effects of freeze drying and convective hot-air drying on predominant bioactive compounds, antioxidant potential and safe consumption of maoberry fruits. LWT. 184:114992. doi:10.1016/j.lwt.2023.114992.
- Köse M, Küçük H, Midilli A. 2024. Microwave effect on drying behavior and quality parameters of green tea leaves. Turk J Electromech Energy. 9(1):33–42.
- Küçük H, Akbulut U, Midilli A. 2022. Single-layer drying modeling of pumpkin (*Cucurbita maxima*). Turk J Electromech Energy. 7(3):110–119.
- Külcü R, Karaaslan S, Varol HT. 2024. Microwave-assisted foam mat drying of pumpkin pulp and development of a new drying model. J Sci Eng Res. 11(3):81–94.
- Kumar A, Kandasamy P, Chakraborty I, Hangshing L. 2022. Analysis of energy consumption, heat and mass transfer, drying kinetics and effective moisture diffusivity during foam-mat drying of mango in a convective hot-air dryer. Biosyst Eng. 219:85–102. doi:10.1016/j.biosystemseng.2022.04.026.
- Kumar D, Ladaniya M, Gurjar M, Kumar S. 2022. Impact of drying methods on natural antioxidants, phenols and flavanones of immature dropped *Citrus sinensis* L. Osbeck fruits. Sci Rep. 12(1):6684. doi:10.1038/s41598-022-10661-7.
- Kusuma HS, Diwiyanto YM, Jaya DEC, Amenaghawon AN, Darmokoeseoemo H. 2023. Evaluation of drying kinetics, electric and emission study of *Musa paradisiaca* L. leaves using microwave-assisted drying method. Appl Food Res. 3(2):100322. doi:10.1016/j.afres.2023.100322.
- Kusuma HS, Sembiring LI, Aisahasnati S. 2023. Microwave-assisted drying of *Cymbogopon nardus* leaves: kinetics, moisture diffusivity, energy, and emission study. J Stor Prod Res. 102:102130. doi:10.1016/j.jspr.2023.102130.
- López-Ortiz A, Méndez-Lagunas L, Delesma C, Longoria A, Escobar J, Muñoz J. 2020. Understanding the drying kinetics of phenolic compounds in strawberries: an experimental and density functional theory study. Innov Food Sci Emerg Technol. 60:102283. doi:10.1016/j.ifset.2019.102283.
- Luka BS, Vihikwagh QM, Ngabea SA, Mactony MJ, Zakka R, Yuguda TK, Adnoui M. 2023. Convective and microwave drying kinetics of white cabbage (*Brassica oleraceae* var *capitata* L.): mathematical modelling, thermodynamic properties, energy consumption and reconstitution kinetics. J Agric Food Res. 12:100605. doi:10.1016/j.jafr.2023.100605.
- Marović R, Badanjak Sabolović M, Brnčić M, Ninčević Grassino A, Kljak K, Voća S, Karlović S, Rimac Brnčić S. 2024. The nutritional potential of avocado by-products: a

- focus on fatty acid content and drying processes. *Foods*. 13(13):2003. doi:10.3390/foods13132003.
- Mokhtarian M, Tavakolipour H, Kalbasi-Ashtari A, Koushki F. 2021. The effects of solar drying on drying kinetics and effective moisture diffusivity of pistachio nut.
- Mouhoubi K, Boulekbache-Makhlouf L, Mehaba W, Himed-Idir H, Madani K. 2022. Convective and microwave drying of coriander leaves: kinetics characteristics and modeling, phenolic contents, antioxidant activity, and principal component analysis. *J Food Process Eng*. 45(1):e13932. doi:10.1111/jfpe.13932.
- Moussa H, Dahmoune F, Hentabli M, Remini H, Mouni L. 2022. Optimization of ultrasound-assisted extraction of phenolic-saponin content from *Carthamus caeruleus* L. rhizome and predictive model based on support vector regression optimized by dragonfly algorithm. *Chemometr Intell Lab Syst*. 222:104493. doi:10.1016/j.chemolab.2022.104493.
- Ng ZX, Than MJY, Yong PH. 2021. *Peperomia pellucida* (L.) Kunth herbal tea: effect of fermentation and drying methods on the consumer acceptance, antioxidant and anti-inflammatory activities. *Food Chem*. 344:128738. doi:10.1016/j.foodchem.2020.128738.
- Nirmaan A, Rohitha Prasantha B, Peiris B. 2020. Comparison of microwave drying and oven-drying techniques for moisture determination of three paddy (*Oryza sativa* L.) varieties. *Chem Biol Technol Agric*. 7(1):1–7. doi:10.1186/s40538-019-0164-1.
- Ovando-Medina VM. 2023. Infrared drying kinetics of *Capsicum annuum* L. var. *glabriusculum* (Piquin pepper) and mathematical modeling. *J Food Process Eng*. 46(7): e14333. doi:10.1111/jfpe.14333.
- Oyinloye TM, Yoon WB. 2020. Effect of freeze-drying on quality and grinding process of food produce: a review. *Processes*. 8(3):354. doi:10.3390/pr8030354.
- Özcan MM, Al Juhaime F, Ahmed IAM, Uslu N, Babiker EE, Ghafoor K. 2020. Effect of microwave and oven drying processes on antioxidant activity, total phenol and phenolic compounds of kiwi and pepino fruits. *J Food Sci Technol*. 57(1):233–242. doi:10.1007/s13197-019-04052-6.
- Parcheta M, Świsłocka R, Orzechowska S, Akimowicz M, Choińska R, Lewandowski M. 2021. Recent developments in effective antioxidants: the structure and antioxidant properties. *Materials*. 14(8):1984. doi:10.3390/ma14081984.
- Pathare PB, Opara UL, Al-Said FA-J. 2013. Colour measurement and analysis in fresh and processed foods: a review. *Food Bioprocess Technol*. 6(1):36–60. doi:10.1007/s11947-012-0867-9.
- Rahman CM, Rashid TA, Alsadoon A, Bacanin N, Fattah P, Mirjalili S. 2023. A survey on dragonfly algorithm and its applications in engineering. *Evol Intel*. 16(1):1–21. doi:10.1007/s12065-021-00659-x.
- Rasooli Sharabiani V, Kaveh M, Abdi R, Szymanek M, Tanaś W. 2021. Estimation of moisture ratio for apple drying by convective and microwave methods using artificial neural network modeling. *Sci Rep*. 11(1):9155. doi:10.1038/s41598-021-88270-z.
- Reis FR, Marques C, de Moraes ACS, Masson ML. 2022. Trends in quality assessment and drying methods used for fruits and vegetables. *Food Control*. 142:109254. doi:10.1016/j.foodcont.2022.109254.
- Saleem H, Khurshid U, Sarfraz M, Ahmad I, Alamri A, Anwar S, Alamri AS, Locatelli M, Tartaglia A, Mahomoodally MF, et al. 2021. Investigation into the biological properties, secondary metabolites composition, and toxicity of aerial and root parts of *Capparis spinosa* L.: an important medicinal food plant. *Food Chem Toxicol*. 155:112404. doi:10.1016/j.fct.2021.112404.
- Shahrajabian MH, Sun W, Cheng Q. 2021. Plant of the Millennium, Caper (*Capparis spinosa* L.), chemical composition and medicinal uses. *Bull Natl Res Cent*. 45(1):1–9. doi:10.1186/s42269-021-00592-0.
- Shen L, Gao M, Zhu Y, Liu C, Wang L, Kamruzzaman M, Liu C, Zheng X. 2021. Microwave drying of germinated brown rice: correlation of drying characteristics with the final quality. *Innov Food Sci Emerg Technol*. 70:102673. doi:10.1016/j.ifset.2021.102673.
- Shen Y, Tang X, Li Y. 2021. Drying methods affect physicochemical and functional properties of quinoa protein isolate. *Food Chem*. 339:127823. doi:10.1016/j.foodchem.2020.127823.
- Shirkole SS, Mujumdar A, Raghavan G. 2023. Drying of foods: principles, practices and new developments. In: *Drying technology in food processing*. UK: Elsevier; p. 3–29.
- Şimşek M, Küçük H, Midilli A. 2021. Experimental investigation and mathematical modeling of microwave thin layer drying behaviour of apricot, kiwi and mint leaves. *Recep Tayyip Erdoğan Üniv Fen Mühendislik Bilim Derg*. 2(2):13–35. doi:10.53501/rteufemud.969314.
- Solchansanj S, Jayas DS. 2020. Drying of foodstuffs. In: *Handbook of industrial drying*. Florida, US: CRC Press; p. 589–625.
- Sun Y, Zhang M, Mujumdar AS, Yu D. 2021. Pulse-spouted microwave freeze drying of raspberry: control of moisture using ANN model aided by LF-NMR. *J Food Eng*. 292: 110354. doi:10.1016/j.jfoodeng.2020.110354.
- Tayıroğlu B, İncedayı B. 2021. Nutritional potential characterization and bioactive properties of caper products. *J Food Process Preserv*. 45(8):e14670. doi:10.1111/jfpp.14670.
- Tepe TK, Kadakal Ç. 2022. Determination of drying characteristics, rehydration properties, and shrinkage ratio of convective dried melon slice with some pretreatments. *Food Process Preserv*. 46(6):e16544. doi:10.1111/jfpp.16544.
- Tepe TK, Tepe B. 2020. The comparison of drying and rehydration characteristics of intermittent-microwave and hot-air dried-apple slices. *Heat Mass Transfer*. 56(11): 3047–3057. doi:10.1007/s00231-020-02907-9.
- Turgay Ö, Esen Y. 2020. Antioxidant, total phenolic, ascorbic acid and color changes of *Ocimum basilicum* L. by various drying methods. *Food Health*. 6(2):110–116. doi:10.3153/FH20012.
- Turkiewicz IP, Wojdyło A, Tkacz K, Lech K, Nowicka P. 2020. Osmotic dehydration as a pretreatment modulating the physicochemical and biological properties of the Japanese quince fruit dried by the convective and

- vacuum-microwave method. *Food Bioprocess Technol.* 13(10):1801–1816. doi:10.1007/s11947-020-02522-w.
- Xu Y, Xiao Y, Lagnika C, Li D, Liu C, Jiang N, Song J, Zhang M. 2020. A comparative evaluation of nutritional properties, antioxidant capacity and physical characteristics of cabbage (*Brassica oleracea* var. *capitata* var L.) subjected to different drying methods. *Food Chem.* 309: 124935. doi:10.1016/j.foodchem.2019.06.002.
- Yahia Y, Benabderrahim MA, Tlili N, Hannachi H, Ayadi L, Elfalleh W. 2020. Comparison of three extraction protocols for the characterization of caper (*Capparis spinosa* L.) leaf extracts: evaluation of phenolic acids and flavonoids by liquid chromatography–electrospray ionization–tandem mass spectrometry (LC–ESI–MS) and the antioxidant activity. *Anal Lett.* 53(9):1366–1377. doi:10.1080/00032719.2019.1706546.
- Yatao Z, Xiaowei B, Lanjun Z, Chenye W, Mengmeng H, Weiquan J. 2021. Anti-inflammatory and analgesic effects of alcohol extracts from capers fruits and N-butanol extracts. *Xinjiang Agric Sci.* 58(1):159.
- Yildiz G. 2022. Color, microstructure, physicochemical, textural and sensory properties with the retention of secondary metabolites in convective-, microwave-and freeze-dried carrot (*Daucus carota*) slices. *Br Food J.* 124(11):3922–3935. doi:10.1108/BFJ-03-2021-0308.
- Yilmaz P, Demirhan E, Özbek B. 2021. Microwave drying effect on drying characteristic and energy consumption of *Ficus carica* Linn leaves. *J Food Process Eng.* 44(10): e13831. doi:10.1111/jfpe.13831.
- Yuan Q, He Y, Xiang P-Y, Huang Y-J, Cao Z-W, Shen S-W, Zhao L, Zhang Q, Qin W, Wu D-T. 2020. Influences of different drying methods on the structural characteristics and multiple bioactivities of polysaccharides from okra (*Abelmoschus esculentus*). *Int J Biol Macromol.* 147: 1053–1063. doi:10.1016/j.ijbiomac.2019.10.073.
- Zheng H, Li Q, Ling Y, Omran M, Gao L, Chen G. 2021. Optimisation on the microwave drying of ammonium polyvanadate (APV)-based on a kinetic study. *J Mater Res Technol.* 13:1056–1067. doi:10.1016/j.jmrt.2021.05.056.
- Zhou Y-H, Pei Y-P, Sutar PP, Liu D-H, Deng L-Z, Duan X, Liu Z-L, Xiao H-W. 2022. Pulsed vacuum drying of banana: effects of ripeness on drying kinetics and physicochemical properties and related mechanism. *LWT.* 161: 113362. doi:10.1016/j.lwt.2022.113362.